

## Electronic supplementary information

### Electron-Delocalization Catalyzer for High Performance Low-temperature Li-S Batteries

Jing Zhang<sup>1</sup>, Lin Li<sup>1</sup>, Mannan Yang<sup>1</sup>, Chen Cheng<sup>1</sup>, Na Tian<sup>1,\*</sup>, Yongzheng Zhang<sup>5</sup>, Dongmao Jiao<sup>1</sup>, Hongzhen Lin<sup>2,\*</sup>, Jian Wang<sup>3,4,\*</sup>

<sup>1</sup> School of Materials Science and Engineering & Faculty of Printing, Packaging Engineering and Digital Media Technology, Xi'an University of Technology, Xi'an 710048, China

<sup>2</sup> *i*-Lab & CAS Key Laboratory of Nanophotonic Materials and Devices, Suzhou Institute of Nano-tech and Nano-bionics, Chinese Academy of Sciences, Suzhou, 215123, China

<sup>3</sup> Helmholtz Institute Ulm (HIU), Ulm D89081, Germany

<sup>4</sup> Karlsruhe institute of Technology, Karlsruhe D76021, Germany

<sup>5</sup> State Key Laboratory of Chemical Engineering, East China University of Science and Technology, Shanghai 200237, China

**Corresponding author:** [tianna@xaut.edu.cn](mailto:tianna@xaut.edu.cn);

[hzlin2010@sinano.ac.cn](mailto:hzlin2010@sinano.ac.cn);

[jian.wang@kit.edu](mailto:jian.wang@kit.edu); [wangjian2014@sinano.ac.cn](mailto:wangjian2014@sinano.ac.cn)

## Experimental Sections

### Synthesis of ODVO@PCN nanocomposites

ODVO@PCN was prepared via a solvothermal method followed by a hydrogen thermal reduction method. In detail, the purified multi-walled carbon nanotubes (CNTs) powder (180 mg) was dispersed into 75 mL deionized water under sonication to form homogeneous suspension, the  $\text{NH}_4\text{VO}_3$  (278.4 mg) was added into 100 mL absolute ethyl alcohol under sonication to form homogeneous solution. The  $\text{NH}_4\text{VO}_3$  solution was then dripped into the dispersion slowly under vigorous stirring. After that, the mixture was transferred into a Teflon-lined stainless-steel autoclave and heated to 180 °C for 24 h. After cooling to room temperature, the resultant solid product was collected by filtration, rinsed by deionized water repeatedly and freezing dried for 24 h. The VO@PCN nanocomposites were obtained by calcining the precursor at 700 °C for 2 h under an Ar (99.99%) atmosphere with a heating rate of 5 °C min<sup>-1</sup>. At last, the ODVO@PCN nanocomposites were generated after heat reduction of the VO@PCN at 500 °C for 2 h under an Ar/H<sub>2</sub> (5%:95%, by volume) mixture atmosphere.

### Preparation of sulfur cathodes nanocomposites

The sulfur cathodes nanocomposites were prepared through in-situ liquid reaction method. The above synthesized ODVO@PCN (200 mg) was suspended in 600 mL deionized water under sonication till form uniform suspension. Sublimed sulfur (0.72 g) with  $\text{Na}_2\text{S}\cdot 9\text{H}_2\text{O}$  (1.82 g) was added into a 25 mL deionized water by stirring at room temperature to obtain  $\text{Na}_2\text{S}_x$  solution. Then, the homogeneous  $\text{Na}_2\text{S}_x$  solution (21 mL) was dripped into the above suspension slowly with strong magnetic stirring. Thereafter, HCOOH solutions (2 mol L<sup>-1</sup>) was added slowly to the  $\text{Na}_2\text{S}_x$  infiltrated ODVO@PCN mixture for in-situ deposition of elemental S with overnight continuous stirring. The as-synthesized mixture was collected by filtration and washed by deionized water to remove the soluble impurities. After freezing dried for 24 h, the collected mixture was sealed in a vessel full of argon gas and heated at 155 °C for 12 h to fully infiltrate sulfur into the porous matrix to generate ODVO@PCN-S nanocomposites. The VO@PCN-S nanocomposites was fabricated using the same method.

### Li-S full cell assembly

Upon a weight ratio of 7:2:1, the sulfur composite cathodes were prepared by mixing the as-synthesized nanocomposites, carbon black, and polyvinylidene fluoride (PVDF) as binder in an appropriate amount of N-methyl-pyrrolidinone (NMP) solvent under continuous stirring till forming uniform slurry. The fully mixed slurry was then coated on aluminum foil to form an even layer by a film blade using a thickness of 200  $\mu\text{m}$ , which was dried in a vacuum oven at 60  $^{\circ}\text{C}$  over 24 h. The prepared electrode was punched into discs of 12 mm in diameter. The Li-S cells were assembled with ODVO@PCN-S discs cathode (12 mm), and Li anode separated by Celgard 2350 commercial separator, adding the electrolyte (1 M LiTFSI with 1 wt%  $\text{LiNO}_3$  dissolved in mixed solvent of DME/DOL in volume ratio of 1:1) according to the electrolyte/sulfur (E/S) ratio of 15  $\mu\text{L mg}^{-1}$ .

### **Materials and cells characterization**

The X-ray diffraction (XRD) was carried out on an XRD-7000S X-ray diffractometer with Cu-K $\alpha$  radiation ( $\lambda=0.15418$  nm) within a  $2\theta$  range of  $10^{\circ}\sim 80^{\circ}$ . X-ray photoelectron spectra (XPS) were collected on an AXIS ULTRA system. Nitrogen absorption and desorption isotherms were recorded on an ASAP 2020 (Micromeritics). Raman spectra were performed on a Horiba Laser Raman spectrometer (EUROVECTOR EA3000). Thermal gravimetric analysis (TGA) was conducted on a TG/DTA 6200 setup with a heating rate of 10  $^{\circ}\text{C min}^{-1}$  under nitrogen flow or air atmosphere. Scanning electron microscopy (SEM) images were observed using a Germany MERLIN Compact Scanning Electron Microscope (Zeiss). Transmission electron microscopy (TEM) samples were imaged using a JEM-3010 Transmission Electron Microscope. The electrochemical impedance spectroscopy (EIS) and cyclic voltammetry (CV) were performed with a VMP-3 potentiostat/galvanostat station. The other electrochemical evaluations on cells were performed on a Neware battery testing system (BTS-5 V 10 mA) within the voltage window of 1.6~2.8 V at different current rates.

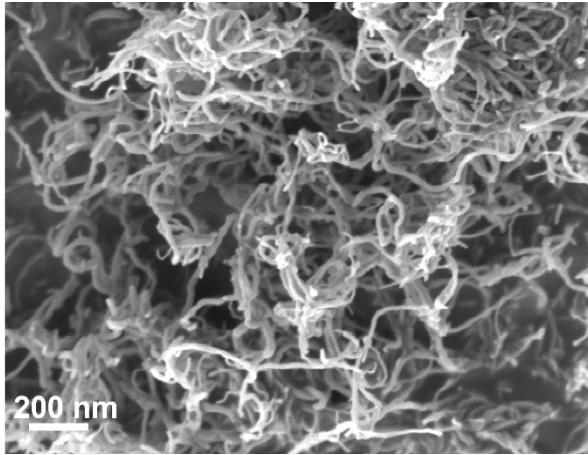


**Figure S1** SEM image of the VO@PCN nanocomposite.

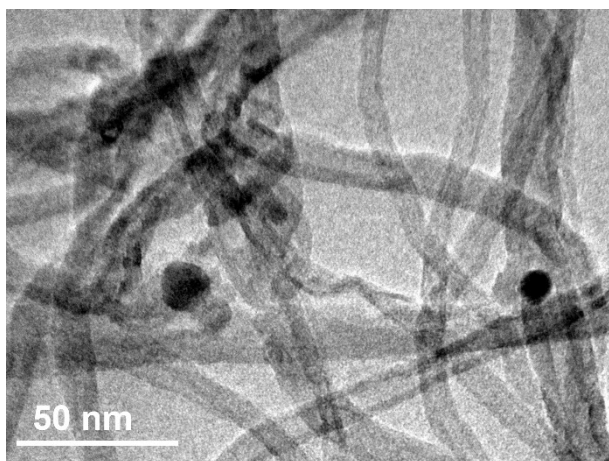


**Figure S2** TEM image of the VO@PCN nanocomposite.

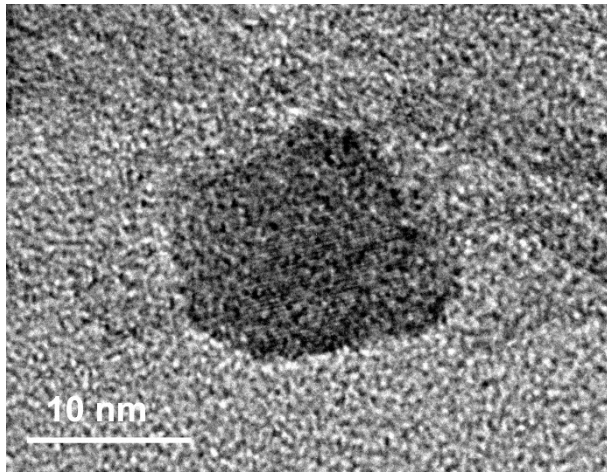


**Figure S3** HRTEM image of the ODVO@PCN nanocomposite.

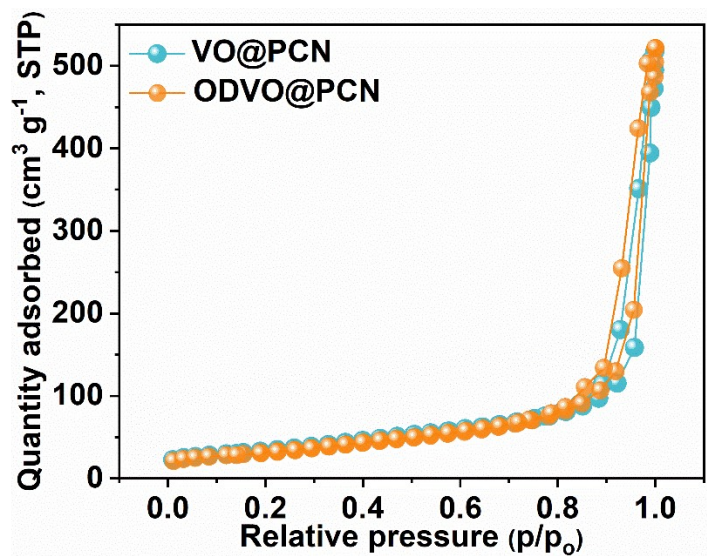


**Figure S4** N<sub>2</sub> adsorption/desorption isotherms of the ODVO@PCN and VO@PCN nanocomposites.

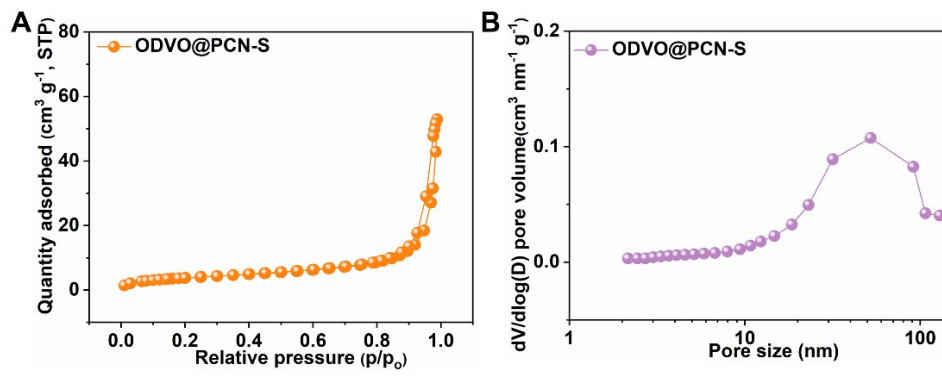


**Figure S5** (A) Nitrogen adsorption/desorption isotherms and (B) pore size distribution of the ODVO@PCN-S nanocomposite.



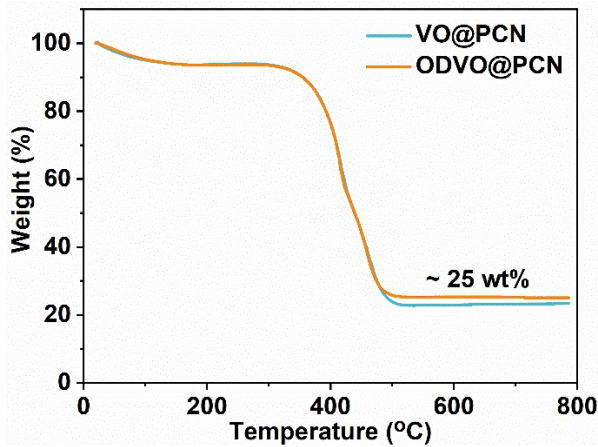
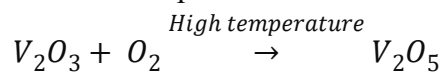


**Figure S6** TGA curves of the ODVO@PCN and VO@PCN nanocomposites.

**Figure S6** displays TGA curves of the ODVO@PCN and VO@PCN nanocomposites under air atmosphere with heating rate of  $10\text{ }^{\circ}\text{C min}^{-1}$ , presenting that the ODVO@PCN experiences a fast weight loss of about 75 wt.% between 300~500  $^{\circ}\text{C}$ . Finally, 25% of the nanocomposite is remained. According to the reaction formula:



In theory, the weight of the pure  $V_2O_3$  increases to nearly 1.21 times due to the transformation from  $V_2O_3$  to  $V_2O_5$  under the high temperature heating with  $O_2$  atmosphere. Therefore, it could be deduced that the remained mass after the TG analysis in **Figure S6** should be ascribed to the final existence of  $V_2O_5$ , which was corresponded to be about 20.6% ( $25\% / 1.21$ ) of  $V_2O_3$ . This experimental result matches quite well with the nominal designed ratio of  $V_2O_3$ .

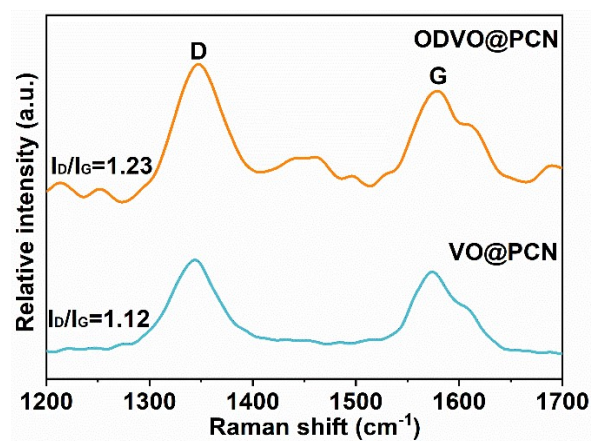


**Figure S7** The D and G peaks in Raman spectra of the ODVO@PCN and VO@PCN nanocomposites.

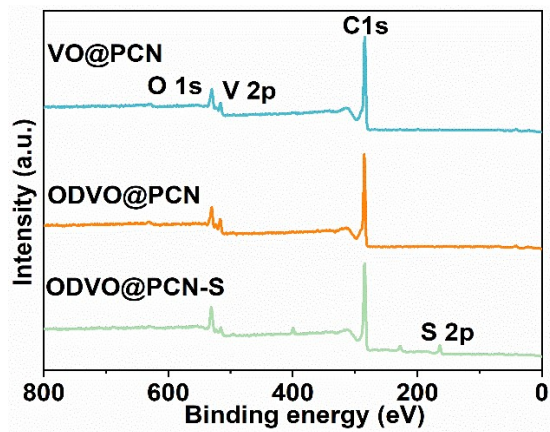


**Figure S8** XPS survey spectra of the ODVO@PCN, ODVO@PCN-S and VO@PCN nanocomposites.

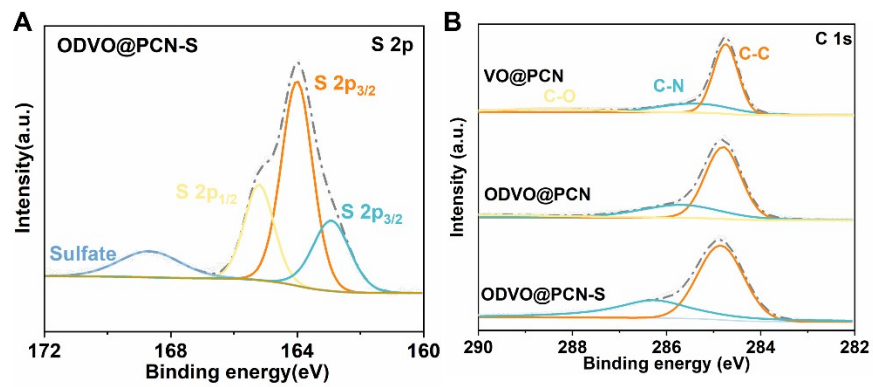


**Figure S9** High-resolution spectra of (A) S 2p of the ODVO@PCN-S nanocomposite and (B) C 1s of the ODVO@PCN, ODVO@PCN-S and VO@PCN nanocomposites.

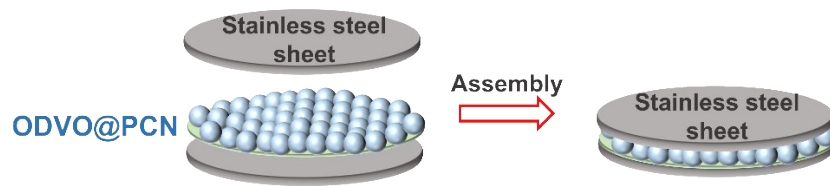


**Figure S10** Schematic depiction of assembly of block cells for the measure of the ionic conductivity.

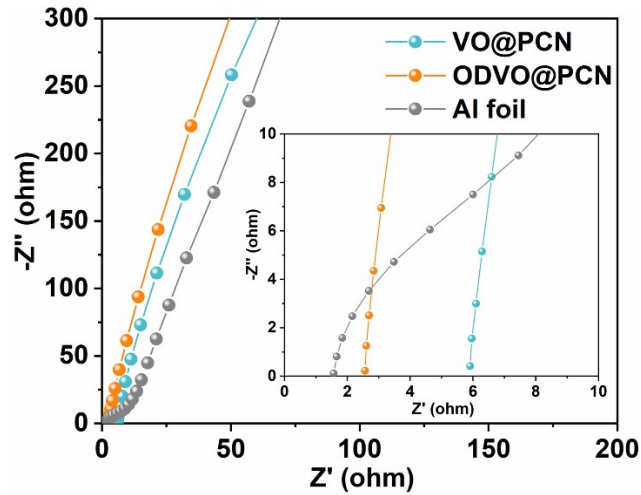


**Figure S11** Electrochemical impedance spectroscopy (EIS) spectra recorded on the block cells with ODVO@PCN and VO@PCN electrode.

In detail, the block cell is assembled by sandwiching ODVO@PCN between two stainless steel sheets (**Figure S10**). Then, the ion conductivity ( $\sigma$ ) was tested on the block cells and calculated on the following formula:

$$\sigma = \frac{L}{R_b S}$$

where L represents the thickness of the modulation layer,  $R_b$  is the resistance of the coating layer recorded by the electrochemical impedance spectroscopy (EIS) spectra in **Figure S11**, and S is the effective area of the layer.

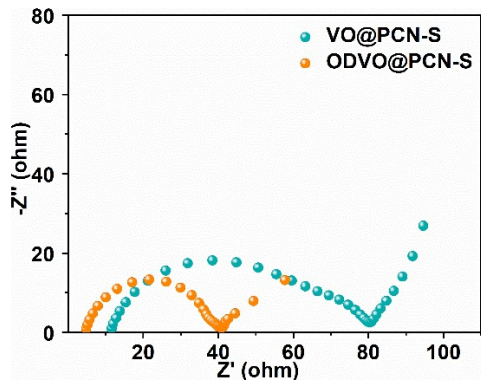


**Figure S12** Comparison of EIS between the ODVO@PCN-S and VO@PCN-S electrodes after cycling.

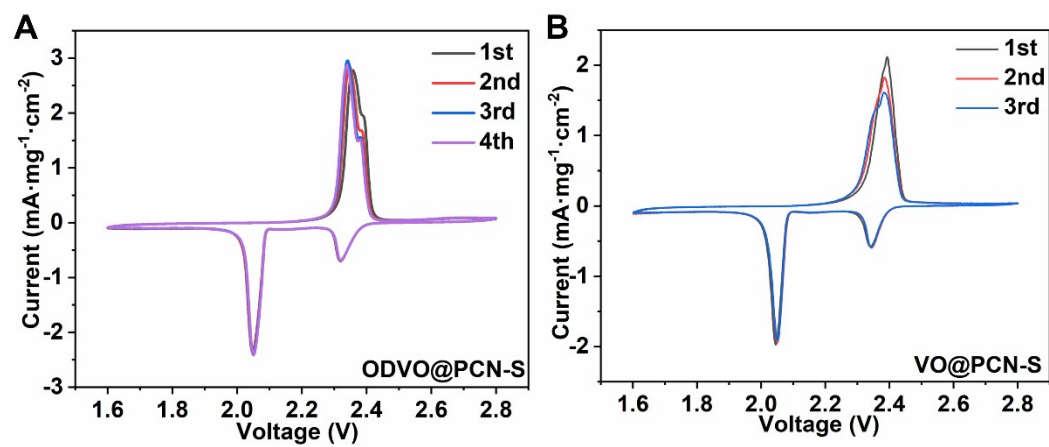


**Figure S13** CV profiles of (A) ODVO@PCN-S and (B) VO@PCN-S cathodes in the first few cycles scanning at 0.1 mV s<sup>-1</sup>.



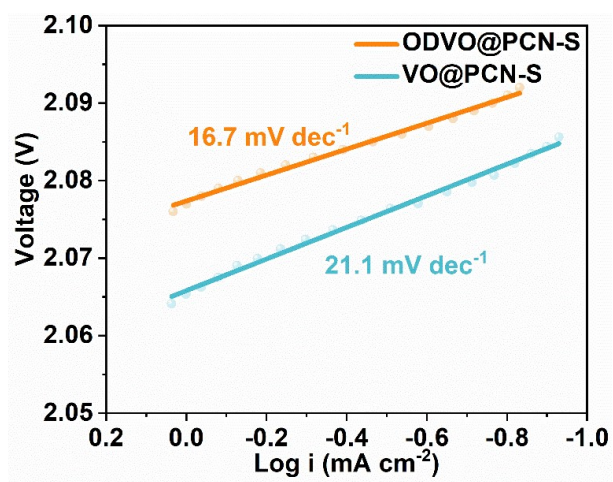


**Figure S14** Tafel plots of different cathodes derived from corresponding initial CV curves at the scan rate of 0.1 mV s<sup>-1</sup>.

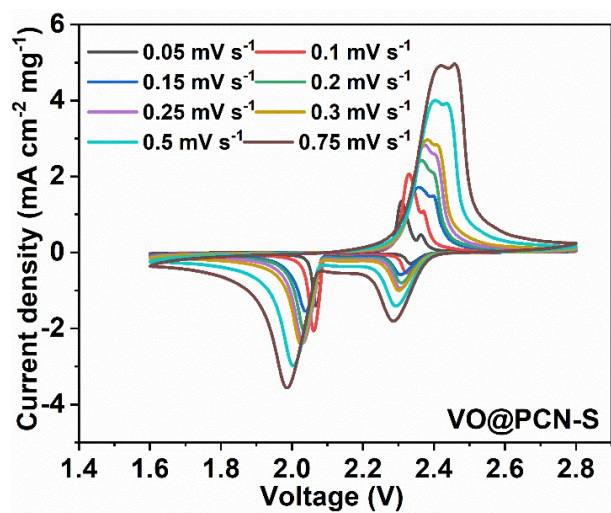


**Figure S15** Scan rate-dependent CV curves on the VO@PCN-S cathode.

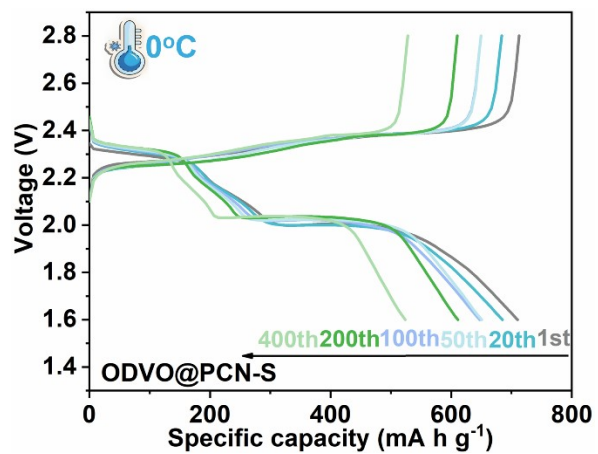


**Figure S16** Voltage-capacity profiles on the ODVO@PCN-S cathode cycled at 0.5 C under 0 °C.

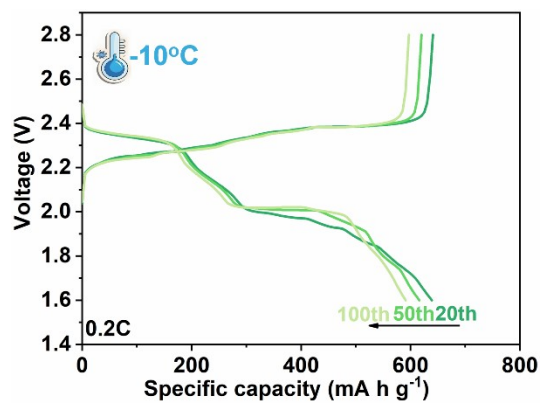


**Figure S17** Voltage-capacity profiles on the ODVO@PCN-S cathode cycled at 0.2 C under -10 °C.

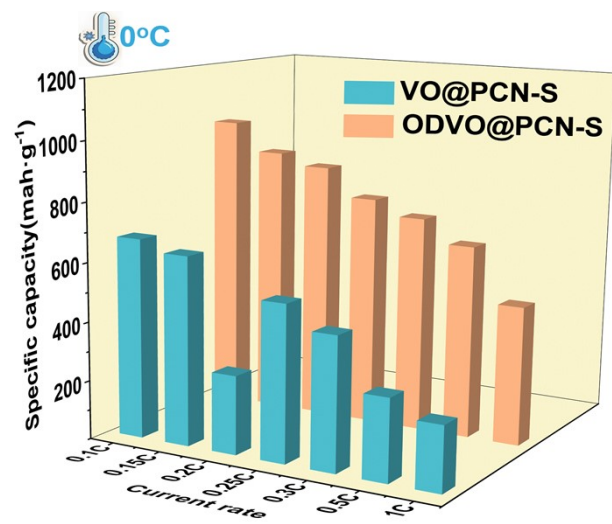


**Figure S18** Capacity comparison on the ODVO@PCN-S and VO@PCN-S cathodes at various current rate under low temperature of 0 °C.

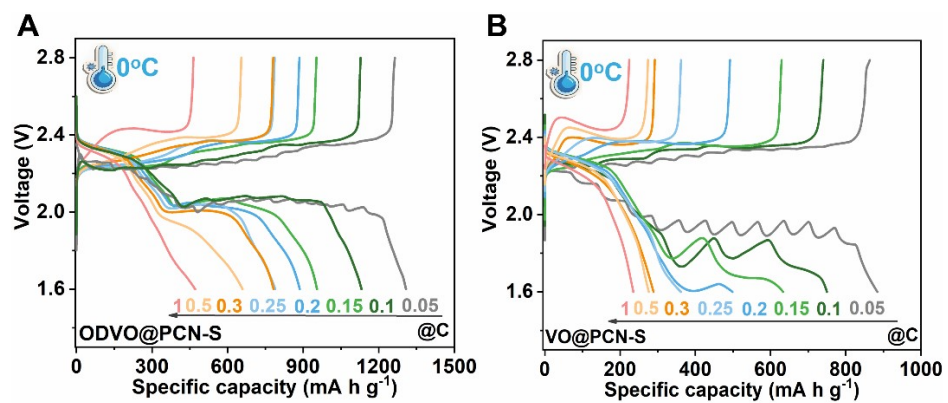


**Figure S19** Voltage-capacity profiles on the ODVO@PCN-S and VO@PCN-S cathodes depending on current rate under low temperature of 0 °C.

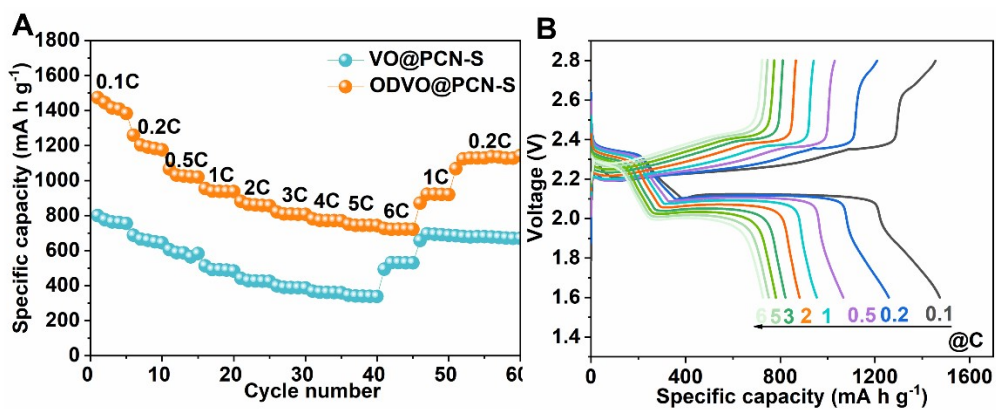


**Figure S20** (A) Rate performance of the two cathodes and (B) Voltage-capacity profiles on the ODVO@PCN-S cathode depending on current rate under room temperature.

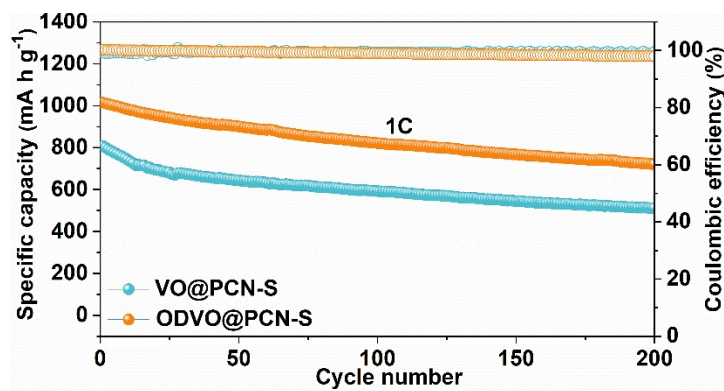


**Figure S21** Cycle performance of the ODVO@PCN-S and VO@PCN-S cathodes at 1C under room temperature.



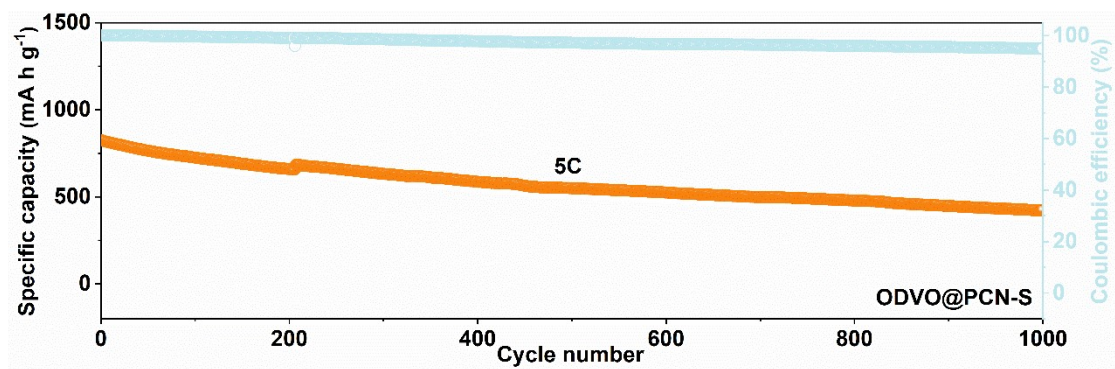


**Figure S22** Cycle performance of the ODVO@PCN-S cathode at 5C under room temperature

**Table S1** Comparison of electrochemical performance of the ODVO@PCN-S cathode with that reported in recent literatures.

Cathodes	Synthesis method	High-rate performance (mA h g <sup>-1</sup> )	Cycling performance and retention	Cycle number	Temperature (°C)	References
<b>ODVO@PCN-S</b>	<b>Hydrothermal reaction and hydrogen treatment</b>	<b>521 (1C)</b>	<b>710 (90.7%, 0.5C) 892 (64.5%, 0.2C)</b>	<b>400 (0.5C) 100 (0.2C)</b>	<b>0 (0.5C) -10 (0.2C)</b>	<b>This work</b>
MB-VN modified separator	Solvothermal method and pyrolysis under NH <sub>3</sub> atmosphere	800 (0.2C)	649 (85.2%, 1C)	100	-10	<i>ACS Nano</i> , 2023, 17, 11527.
Mo <sub>6</sub> S <sub>8</sub> /S	Ball milling	800 (0.2C)	/	/	0	<i>Small</i> , 2023, 19, 2300042.
EPDB-CgCP	Chemical assembly with phosphorization reaction in Ar atmosphere	/	972 (66.6%, 0.1C)	80	0	<i>Adv. Funct. Mater.</i> , 2023, 33, 2302624.
Ni@C/graphene modified separator	Hydrothermal reaction and Argon gas treatment	/	403 (87.8%, 0.1C)	200	-40	<i>Adv. Energy Mater.</i> 2020, 10, 2000907.
Li <sub>2</sub> S <sub>6</sub> /FCN-MO@CNFs	Impregnation and pyrolysis under Ar/H <sub>2</sub> atmosphere	278.7 (10C)	1000 (90.5%, 0.2C)	100	-10	<i>Chem. Eng. J.</i> , 2023, 458, 141445.
TiO <sub>2</sub> @C@CSC	Hydrothermal reaction and H <sub>2</sub> /Ar treatment	138 (1C)	649 (51%, 0.2C)	250	-20	<i>ACS Sustain. Chem. Eng.</i> , 2023, 11, 3657.
PAN@S	Pyrolysis under N <sub>2</sub> atmosphere	/	453 (99.2%, 0.1C)	50	-10	<i>J. Energy Chem.</i> , 2020, 51, 154.